Acta Polytechnica CTU Proceedings **1**(1): 222–226, 2014 doi: 10.14311/APP.2014.01.0222

X-Ray and Near-Infrared Spectroscopy of Dim X-Ray Point Sources Constituting the Galactic Ridge X-Ray Emission

Kumiko Morihana[1], Masahiro Tsujimoto[2], Ken Ebisawa[2]

[1] *Nishiharima Astronomical Observatory, Center for Astronomy, University of Hyogo, 407-2 Nishigaichi, Sayo-cho, Sayo-gun, Hyogo, 679-5313, Japan*

[2] *Japan Astrospace Exporation Agency, Institute of Space and Astronautical Science, 3-1-1 Yoshino-dai, Chuo-ku, Sagamihara, Kanagawa 252-5210, Japan*

Corresponding author: morihana@nhao.jp

Abstract

We present the results of X-ray and Near-Infrared observations of the Galactic Ridge X-ray Emission (GRXE). We extracted 2,002 X-ray point sources in the *Chandra* Bulge Field (l =0°.113, b = 1°.424) down to $\sim 10^{-14.8}$ ergs cm^{-2} s^{-1} in 2–8 keV band with the longest observation (∼900 ks) of the GRXE. Based on X-ray brightness and hardness, we classified the X-ray point sources into three groups: A (hard), B (soft and broad spectrum), and C (soft and peaked spectrum). In order to know populations of the X-ray point sources, we carried out NIR imaging and spectroscopy observation. We identified ∼11% of X-ray point sources with NIR and extracted NIR spectra for some of them. Based on X-ray and NIR properties, we concluded that non-thermal sources in the group A are mostly active galactic nuclei and the thermal sources are mostly white dwarf binaries such as cataclysmic variables (CVs) and Pre-CVs. We concluded that the group B and C sources are X-ray active stars in flare and quiescence, respectively.

Keywords: galaxy: bulge - galaxy: disk - IR - X-rays.

1 Introduction

Since the dawn of the X-ray astronomy, an apparently diffuse emission of low surface brightness has been known to exist along the Galactic Plane (GP; $|l|$ <45°, $|b|$ <1°), which is referred to as the Galactic Ridge X-ray emission (GRXE; e.g.,Worral et al. 1982; Warwick et al., 1985). The X-ray spectrum is characterized by hard continuum with a strong 6.7 keV Fe K emission line (Koyama et al., 1986a). The origin of the GRXE had been a mystery for a long time. A long-standing debate had been whether it is a truly diffuse plasma (Ebisawa et al., 2001, 2005) or a sum of unresolved X-ray point sources (Revnivtsev et al. 2006). Recently, Revnivtsev et al (2009) showed that ∼80% of the Fe K emission line was resolved into dim point sources using the deepest X-ray observations (∼900ks) made with the *Chandra* at a slightly off-plane region of (l, b)=(0°.113, –1°.424) in the Galactic bulge (*Chandra* bulge field; hereafter, CBF).

If the GRXE is composed of the dim X-ray point sources, new questions arise. *What are the populations of the dim X-ray point sources? Which class of sources contribute to the Fe K emission line?* We do not know the population of majority of the dim point sources due to a limited number of X-ray photons. Thus, we focus on Near-Infrared (NIR), which has almost the same penetrating power as X-rays into deep interstellar extinction toward the GP.

We studied the population constituting the GRXE combining X-ray data with NIR data in this paper. In particular, we focus on the population contribute to the Fe K line of the GRXE spectrum.

2 Analysis and Results

2.1 X-ray

2.1.1 Observation and source extraction

We retrieved 10 archived data of the CBF taken with the Advanced CCD Imaging Spectrometer (ACIS)-I array on board *Chandra* with a total exposure time of ∼900 ks. We merged 10 data set and extracted 2,002 valid point sources down to $\sim 10^{-14.8}$ ergs cm^{-2} s^{-1} in 2–8 keV (Figure 1). For all the sources, we extracted source and background events.

2.1.2 Spectral fittings

For the *bright* sources (source counts>100), we constructed the background-subtracted spectra and generated instrumental response files. We carried out spectra fittings with thermal (`apec`; Smith et al. 2001) and

non-thermal models (`power-law`) for the *bright* sources. As the results, 11 *bright* sources with more than 1000 counts have hard power-law like hard spectra with the photon index $\Gamma\sim1.5$.

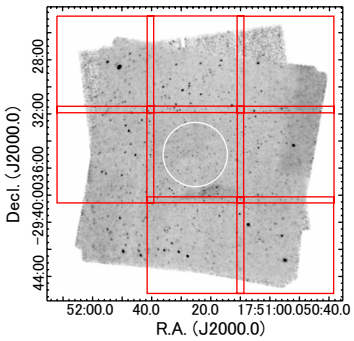

Figure 1: Smoothed and exposure-corrected X-ray image of the CBF (0.5–8 keV). The field of view of the SIRIUS (NIR) observations are shown by red squares. The white circle shows the region, the result of which was published in Revnivtsev et al (2009).

2.1.3 Grouping

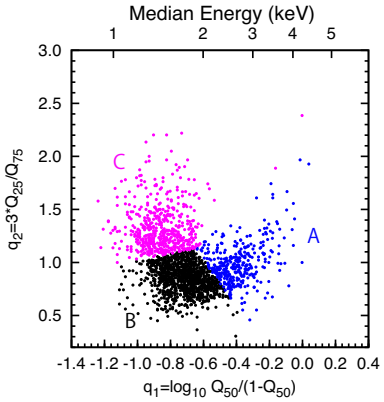

Figure 2: X-ray color-color diagram of all detected X-ray sources. The converted median energy is shown in the upper x-axis. Color difference shows groups defined in § 2.1.3.

We constructed an X-ray color-color diagram (Hong et al., 2004) using the quantiles (E_{25}, E_{50}, and E_{75}) characterizing the spectral shape of each source (Figure 2). Here, E_x (keV) is the energy below which x% of photons reside in the energy-sorted event list. E_{50} is equivalent to the median energy (The details are in Morihana et al., 2013). Here, the q_1 value indicates the degree of photon spectrum being biased toward the higher ($q_1 > 0$) or lower ($q_1 < 0$) energy end (hard or soft spectra), and the q_2 value indicates the degree of photon spectrum being less ($q_2 > 1$) or more ($q_2 < 1$) concentrated around the peak (broad or narrow spectra). Based on the X-ray color-color diagram, we classified all the point sources into three groups, which are the group A (hard), B (soft and brooded spectrum), and the group C (soft and peaked spectrum).

2.1.4 Global spectral fittings

Furthermore, we performed global spectral fittings in 0.5–8 keV for the composite spectrum for each group in a similar manner in § 2.1.2 (Figure 4).

For the group A spectrum, neither a power-law nor a thin-thermal plasma model reproduced the spectrum well, respectively because of the excess emission at 6.7 keV or a flatness of the continuum. So we fitted the spectrum with a combination of the two models, which was successful. The equivalent width (EW) of the Fe K feature becomes larger as the flux decreases (Figure3), which suggest that the thermal component becomes strong against the non-thermal component as the flux decreases.

For the group B spectrum, several emission lines are seen, including the 6.7 keV emission line from Fe_{XXV} and 2.5 keV from S_{XV}. This set of emission lines indicates a multiple-temperature plasma, and indeed the spectrum was reproduced well with two thin-thermal plasma components, but not with one component.

For the group C spectrum, several emission lines are also seen. Unlike the group B sources, the Fe_{XXV} emission at 6.7 keV is absent. We fitted the spectrum using the same model with group B.

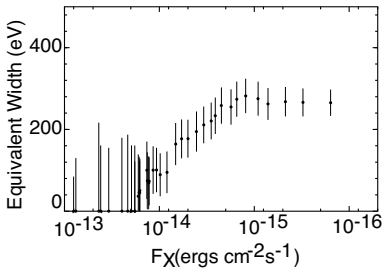

Figure 3: Equivalent width of the Fe K line against the decreasing flux in 2-8 keV above which the cumulative combined spectra in the group A were constructed. The 1σ statistical uncertainty is shown for each data.

2.2 NIR Imaging

2.2.1 Observation and source extraction

To identify the X-ray point sources with NIR, we carried out NIR observations using Simultaneous Infrared for Unbiased Survey (SIRIUS; Nagayama et al., 1999) on the InfraRed-Survey Facility (IRSF) 1.4 m telescope

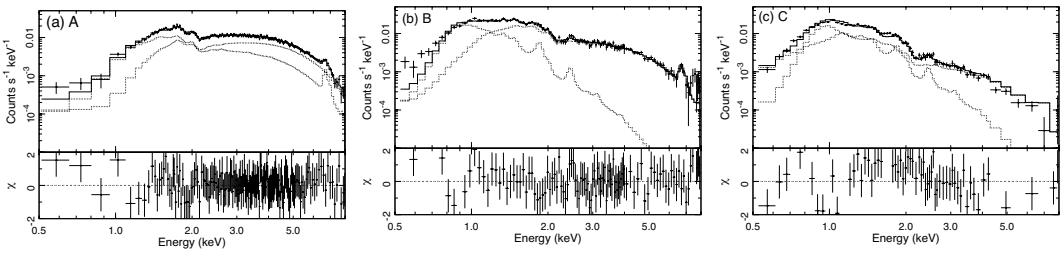

Figure 4: Composite spectra and the best-fit global model of the group (a) A, (b) B, and (c) C. The lower panel shows the residuals of the data to the fit. The best-fit parameters can be found in Table 1.

Table 1: Best-fit Parameters for Global Spectral Model in 0.5–8.0 keV

Group	$N_{\rm H}{}^{(1)}$[1] (10^{22} cm^{-2})	$k_{\rm B}T^{(1)}$[2] (keV)	$N_{\rm H}{}^{(2)}$ (10^{22} cm^{-2})	$k_{\rm B}T^{(2)}$ (keV)	Z[3]	Γ[4]	χ^2/d.o.f.
A	$1.09^{+0.39}_{-0.50}$	$6.65^{+3.24}_{-3.03}$	$2.46^{+2.35}_{-0.58}$	...	$0.97^{+0.36}_{-0.32}$	$1.29^{+0.18}_{-0.40}$	205.36/504
B	$0.75^{+0.06}_{-0.05}$	$0.74^{+0.54}_{-0.45}$	$0.80^{+0.22}_{-0.18}$	$7.87^{+1.86}_{-4.84}$	$0.99^{+0.33}_{-0.29}$	...	98.68/103
C	$0.70^{+0.18}_{-0.11}$	$0.78^{+0.04}_{-0.03}$	$0.04^{+0.05}_{-0.04}$	$4.50^{+0.65}_{-0.35}$	$0.15^{+0.16}_{-0.12}$	...	85.86/102

[1]Interstellar extinction column density for the first component (the lower temperature component for the two-temperature model. [2]Plasma temperature for the second component (the higher temperature component for the two-temperature model). [3]Metal abundance relative to the solar value for the thermal component. [4]Photon index for the power-law model as the second component.

in South Africa Astronomical Observatory. We covered the CBF as we show in Figure 1. We extracted NIR source with a 3σ level using sextractor version 2.8.6, which are 52312 (J), 61,188 (H), and 65,051 ($K_{\rm s}$) sources down to $K_{\rm s}\sim$16 mag. For asymmetry and photometry correction, we rendered the Two Micron All Sky Survey (2MASS) point source catalog. For asymmetry, the SIRIUS positions are determined at an accuracy of the pixel size of SIRIUS (0.45″).

2.2.2 Cross correlation

We search for possible NIR counterparts for all the X-ray point sources using 2MASS and the SIRIUS. We searched NIR counterpart sources within 1σ error circle (X-ray-2MASS source; 1.3″, X-ray-SIRIUS source; 1.2″). When there are two or more sources within the 1σ circle, we assumed the closest one to be the counterpart. Then, we finally recognized 222 X-ray sources to have NIR counterpart within 1σ circle ($\sim$11% of all the X-ray point sources).

2.3 NIR spectroscopy

We conducted NIR spectroscopy observation for some selected objects in the CBF using Subaru/Multi-Object InfraRed Camera and Spectrograph (MOIRCS). We selected 51 sources for spectroscopy in $K_{\rm s}$-band based on X-ray hardness and source variability. Figure 5 shows examples of NIR spectrum. We finally obtained 33 NIR spectra of the X-ray point source in the CBF. Combined X-ray results, there are two type of sources in the CBF, which are (1) Sources with HI (Brγ) and CO absorption features in NIR spectra and hard X-ray spectra, (2) sources only with CO absorption features in NIR spectra and soft X-ray spectra. From these properties, type (1) sources are K or M spectral type stars and type (2) sources are M spectral type stars.

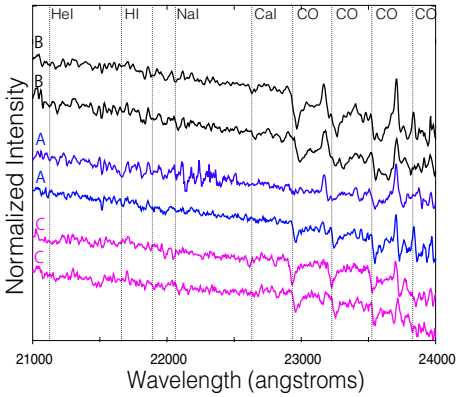

Figure 5: Examples of $K_{\rm s}$-band spectra in the CBF. Upper label of each spectrum shows groups in § 2.1.3 defined by X-ray properties.

3 Discussions & Conclusion

We now discuss likely populations in each group based on the results presented above. The transition from one class to another is continuous along the color and flux, so the groups are naturally a mixture of sources of different classes.

First, we consider that the group A sources are mostly mixture of active galactic nuclei (AGNs) and white dwarfs (WDs) binaries, each responsible for the power-law and thermal plasma components in the composite spectrum (Figure 4). In the spectral fitting, the power-law component has a spectral index of $1.29^{+0.18}_{-0.40}$, which is similar to the typical spectral form of AGNs (Table 1 e.g.; Rosati et al., 2002). For the thermal component of the composite spectrum of the group A, a strong Fe K feature and 6.7 keV plasma temperature are seen. Both of these features are observational characteristics of magnetic CVs (Ezuka & Ishida 1999). Other classes of WD binaries, such as dwarf novae, pre-CVsmay also considered for the likely classes. Pre-CVs are poorly recognized class of sources, which are detached binaries of a WD and a late-type star, unlike conventional CVs that are semi-detached systems. Some of them show strong Fe K emission in the hard X-rays (Matranga et al. 2012). In fact, showed near-infrared spectra of selected X-ray sources presented in this paper, in which some thermal A sources do not exhibit the Brγ emission that is typical for the conventional CVs (Dhillon et al. 1997). We thus consider that pre-CVs, most of which do not show the Brγ emission (Howell et al. 2010; Schmidt& Mikoajewska 2003), also account for at least some fraction of the thermal source population in the group A.

The group B and C sources are Galactic sources with a soft thermal spectrum, and we consider that most of them are likely to be X-ray active stars. The composite spectra of these two groups were fitted with two plasma components. In these groups, the spectra type of the sources are K- or M-type spectra, which has no Brγ emission line. We speculate that the differences between B and C is that most C sources represent active binary stars in the quiescence, while most B sources represent those during flares. From these things, we consider that the group B and C sources are X-ray active stars in flare and quiescence, respectively.

Acknowledgement

This research has made use of public data obtained from *Chandra*X-ray Center which is operated for NASA by the Smithsonian Astrophysical Observatory. This work has also made use of software from High Energy As astrophysics Science Archive Research Center (HEASAC) which is provided by NASA Goddard Space Flight Center.

References

[1] Dhillon, V. S., Marsh, T. R., Duck, S. R., & Rosen, S. R. 1997, MINAREAS, 285, 95

[2] Ebisawa, K., Maeda, Y., Kaneda, H., & Yamauchi, S. 2001, Science, 293, 1633 doi:10.1126/science.1063529

[3] Ebisawa, K., Tsujimoto, M., Paizis, A., et al. 2005, ApJ, 635, 214 doi:10.1086/497284

[4] Ezuka, H. & Ishida, M. 1999, ApJS, 120, 277

[5] Hong, J., Schlegel, E. M., & Grindlay, J. E. 2004, ApJ, 614, 508 doi:10.1086/423445

[6] Koyama, K., Makishima, K., Tanaka, Y., & Tsunemi, H. 1986, PASJ, 38, 121

[7] Matranga, M., Drake, J. J., Kashyap, V., & Steeghs, D. 2012, ApJ, 747, 132 doi:10.1088/0004-637X/747/2/132

[8] Morihana, K., Tsujimoto, M., Yoshida, T., & Ebisawa, K. 2013, ApJ, 766, 144M doi:10.1088/0004-637X/766/1/14

[9] Nagayama, T., et al., 2003, in Society of Photo-Optical Instrumentation Engineers (SPIE) Conference Series, Vol. 4841, M. Iye & A. F. M. Moorwood, 459–464

[10] Revnivtsev, M., Sazonov, S., Gilfanov, M., Churazov, E., & Sunyaev, A&A, 452, 169R

[11] Revnivtsev, M., Sazonov, S., et al., 2009, Nature, 458,1142 doi:10.1038/nature07946

[12] Rosati, P., Tozzi, P.,et al. 2002, ApJ, 566, 667 doi:10.1086/338339

[13] Schmidt, M. R., & Mikołajewska, J. 2003, Near-Infrared Spectra of a Sample of Symbiotic Stars

[14] Smith, R. K., Brickhouse, N. S., Liedahl, D. A., & Raymond, J. C. 2001, ApJl, 556, L91 doi:10.1086/322992

[15] Warwick, R. S., Turner, M. J. L., Watson, M. G., & Willingale, R. 1985, Nature, 317, 218 doi:10.1038/317218a0

[16] Worrall, D. M., Marshall, F. E., Boldt, E. A., & Swank, J. H. 1982, ApJ, 255, 111

DISCUSSION

Takeshi Go Turu's Comment: Is the Fe line a mixture of Fe lines (6.4, 6.7 7.0 keV) or 6.7 keV line?

The Fe line in our GRXE spectrum is a mixture of the Fe lines (6.4, 6.7, and 7.0 keV). The line center of the Fe line is $\sim$6.7 keV.

Guainazzi Matteo's Comment: Radio-quiet AGNs normally exhibit iron Kα lines. This may suggest that your iron free AGNs could be orimary radio-loud. Do you have radio measurements, that could validate this hypothesis?

I consider that Fe K line of most background AGNs are red-shifted, because most background AGNs constituting the GRXE are at far distance.